Available online at www.sciencedirect.com

ScienceDirect

www.elsevier.com/locate/jes

JES JOURNAL OF ENVIRONMENTAL SCIENCES

www.jesc.ac.cn

# Reuse of Fenton sludge as an iron source for $NiFe_2O_4$ synthesis and its application in the Fenton-based process

*Hui Zhang[1,**], Jianguo Liu[1,**], Changjin Ou[1], Faheem[1], Jinyou Shen[1,*], Hongxia Yu[1], Zhenhuan Jiao[2], Weiqing Han[1], Xiuyun Sun[1], Jiansheng Li[1], Lianjun Wang[1,*]*

1. *Jiangsu Key Laboratory of Chemical Pollution Control and Resources Reuse, School of Environmental and Biological Engineering, Nanjing University of Science and Technology, Nanjing 210094, China*
2. *Beijing Changping Water Authority, Beijing 102200, China*

ARTICLE INFO

*Article history:*
Received 24 January 2016
Revised 28 March 2016
Accepted 18 May 2016
Available online 3 June 2016

*Keywords:*
Fenton
Iron-containing sludge
Reuse
Nickel ferrite
Magnetic catalyst

ABSTRACT

The potentially hazardous iron-containing sludge from the Fenton process requires proper treatment and disposal, which often results in high treatment cost. In this study, a novel method for the reuse of Fenton sludge as an iron source for the synthesis of nickel ferrite particles ($NiFe_2O_4$) is proposed. Through a co-precipitation method followed by sintering at 800°C, magnetic $NiFe_2O_4$ particles were successfully synthesized, which was confirmed by powder X-ray diffraction (XRD), scanning electronic microscopy (SEM), energy dispersive spectroscopy (EDS), Fourier transform infrared spectroscopy (FT-IR) and Raman spectroscopy. The synthesized $NiFe_2O_4$ could be used as an efficient catalyst in the heterogeneous Fenton process. In phenol degradation with $H_2O_2$ or $NiFe_2O_4$ alone, the phenol removal efficiencies within the reaction time of 330 min were as low as 5.9% ± 0.1% and 13.5% ± 0.4%, respectively. However, in the presence of both $NiFe_2O_4$ and $H_2O_2$, phenol removal efficiency as high as 95% ± 3.4% could be achieved, indicating the excellent catalytic performance of $NiFe_2O_4$ in the heterogeneous Fenton process. Notably, a rapid electron exchange between $\equiv Ni^{II}$ and $\equiv Fe^{III}$ ions in the $NiFe_2O_4$ structure could be beneficial for the Fenton reaction. In addition, the magnetic catalyst was relatively stable, highly active and recoverable, and has potential applications in the Fenton process for organic pollutant removal.



## Introduction

The Fenton process, which is based on the generation of hydroxyl radicals (HO.) from hydrogen peroxide ($H_2O_2$) in the presence of $Fe^{2+}$, has been extensively studied and successfully applied for the effective treatment of various industrial wastewaters (Bautista et al., 2008; Pignatello et al., 2006). However, despite its simplicity, the main weakness of the Fenton process is the formation of sludge during neutralization after Fenton oxidation (Ma and Xia, 2009). The yield of Fenton sludge is dependent upon the ratio and volume of the added reagents. Due to the residual of toxic organics or heavy metals in it, sludge from the Fenton process treating recalcitrant industrial wastewater is often disposed as hazardous solid waste, which leads to high sludge disposal cost and the risk of secondary pollution. Therefore, Fenton sludge is the main obstacle preventing full

* *Corresponding authors*. E-mail addresses: shenjinyou@mail.njust.edu.cn (J. Shen), wanglj@mail.njust.edu.cn (L. Wang).
** *The authors contribute equally to this study.*

http://dx.doi.org/10.1016/j.jes.2016.05.010
1001-0742/

scale application of the Fenton process in the field of industrial wastewater treatment (Bautista et al., 2008).

To minimize the production of Fenton sludge, two approaches have been suggested, i.e., development of heterogeneous catalysts and reuse of iron in the sludge. Various heterogeneous catalysts have been developed, such as natural minerals (Garrido-Ramirez et al., 2010), iron-containing clays (Navalon et al., 2010), iron immobilized on solid support (Aleksić et al., 2010) and zero-valent iron (Shen et al., 2013; Liu et al., 2015). Heterogeneous catalysts are superior to the traditional homogeneous catalyst, i.e., $Fe^{2+}$, due to the easy separation of the catalysts from the treated wastewater by sedimentation or an external magnetic field (Liu et al., 2012). Therefore, generation of Fenton sludge in a heterogeneous Fenton system can be reduced to some extent. However, the catalytic activity is usually deteriorated after repetitive use due to the leaching of active iron (Ji et al., 2011) or the decay of active catalytic sites (Takbas et al., 2008). Recently, reuse of iron-containing Fenton sludge has been drawing increasing interest from researchers world-wide. Yoo et al. (2001) suggested the recycling of sludge generated from Fenton oxidation in a coagulation process. With the recycling of Fenton sludge, the sludge to be disposed could be reduced up to 50% and the coagulant could be reduced by 50%. Sheu and Weng (2001) developed a recycling system based on the reduction of $Fe^{3+}$ by $H_2O_2$ to produce $Fe^{2+}$, which could be used as a Fenton reagent. Bolobajev et al. (2014) developed a sequential Fenton/Fenton-based system for the treatment of landfill leachate. Iron-containing sludge produced from the Fenton process could be reused as an iron source in the following Fenton-based system, thus production of hazardous ferric waste could be minimized. Cao et al. (2009) presented a simple method for recovering the iron catalyst from the iron hydroxide sludge for oxidative treatment of industrial wastewaters. The sludge was dewatered, dried and baked at 350–400°C, and then the residual solids were dissolved in sulfuric acid to form a reusable catalyst for Fenton and Fenton-like reactions. The reuse routines mentioned above are beneficial for the reduction and minimization of iron-containing sludge compared with traditional treatment processes. However, they increase the overall cost and operational difficulty because of the low utilization efficiency or additional sludge regeneration step. In addition, a feasible method for final and thorough disposal of Fenton sludge has not been suggested so far. Resourcization of Fenton sludge in order to achieve final and thorough disposal merits investigation.

Recently, ferrites, such as $NiFe_2O_4$, $CuFe_2O_4$ and $ZnFe_2O_4$, have drawn much more attention due to their potential application in the fields of catalysis (Rashad and Fouad, 2005), high sensitivity gas sensors (Rezlescu et al., 2006), magnetic fluids (Hasmonay et al., 2000) and microwave devices (Giannakopoulou et al., 2002). Saito et al. (1998) suggested that ferrites could be synthesized by using ferric salts as raw material. Recently, ferrite has been used as the catalyst for heterogeneous photo-Fenton or Fenton-like processes (Liu et al., 2012; Minella et al., 2014). However, to the best of our knowledge, preparation of ferrite using Fenton sludge as an iron source and application of the obtained ferrite as a Fenton catalyst have not yet been reported.

In this work, a new reuse method for Fenton sludge was investigated. The iron-containing Fenton sludge was used as an iron source for the synthesis of nickel ferrite ($NiFe_2O_4$), which was used as a catalyst in the Fenton process. Thus, the objectives of this study were: (1) to synthesize and to characterize $NiFe_2O_4$, (2) to evaluate the catalytic properties and stability of the synthesized $NiFe_2O_4$, and (3) to propose a possible catalytic mechanism for the Fenton process using $NiFe_2O_4$ as catalyst.

## 1. Experimental

### 1.1. Characterization of Fenton sludge

The iron-containing sludge derived from the Fenton process was characterized as follows. The chemical oxygen demand (COD) value was found to be 6500 ± 500 mg/L. The total iron content of the sludge was as high as 7.67 ± 1.87 g/L, which provided a rich iron source for the synthesis of $NiFe_2O_4$. The ratio of volatile solids (VS) to total solids (TS) was 90.46% ± 2.43%, indicating the presence of abundant organics in the sludge. In addition, the iron-containing sludge was fluidized, with water content and total solid content of 89.65% ± 1.75% and 10.35% ± 1.75%, respectively.

### 1.2. Synthesis of $NiFe_2O_4$ from Fenton sludge

$NiFe_2O_4$ particles were synthesized according to the controlled co-precipitation method (Kulkarni et al., 2014). Before the synthesis process, the iron content in the Fenton sludge was determined. $Ni(NO_3)_2$ was dissolved into ultrapure water, and then $Ni(NO_3)_2$ solution was added and mixed into the Fenton sludge at Fe/Ni mole ratio of 2:1. Then 4 mol/L sodium hydroxide solution was added dropwise into the mixture of Fenton sludge and $Ni(NO_3)_2$ to adjust the pH value to 9.0–10.0. During this procedure, the mixture was continuously stirred using a magnetic agitator and kept at a temperature of 50°C. Six hours later, the resultant precipitate was filtered and washed with ultrapure water until the pH value of the filtrate reached 7.0. The solid product was dried in a vacuum oven at 100°C for 8 hr and then sintered at 800°C for 6 hr. The obtained particles were ground and stored for further characterization and application.

### 1.3. Application of $NiFe_2O_4$ in heterogeneous Fenton process

The heterogeneous Fenton reaction for phenol degradation was performed in 100 mL centrifuge tubes containing 50 mL phenol solution. The initial phenol concentration and the initial pH of the phenol solution were 250 mg/L and 3.0, respectively. Then $H_2O_2$ and the obtained $NiFe_2O_4$ powder were added at dosages of 120 mmol/L and 2.0 g/L to initiate the Fenton reaction. The Fenton reaction was carried out on a rotary shaker at 25°C and 200 r/min. After Fenton reaction, $NiFe_2O_4$ was collected by magnetic separation for possible reuse. The control reactions carried out with $NiFe_2O_4$ but without $H_2O_2$ or with $H_2O_2$ but without $NiFe_2O_4$ were performed in the same manner.

### 1.4. The role of the leached iron ions in Fenton process

To evaluate the contribution of homogeneous Fenton oxidation catalyzed by the leached iron ions in the phenol degradation process, the role of the leached iron ions was investigated. After

the first run of the Fenton reaction, the $NiFe_2O_4$ catalyst was separated using an external magnetic field, and 45 mL of the filtrate solution was collected. Subsequently, 5 mL of a solution containing 2500 mg/L phenol was added to 45 mL of the filtrate to form a 50 mL solution, which contained 250 mg/L phenol. 120 mmol/L $H_2O_2$ was then added into this 50 mL solution to initiate the homogeneous Fenton reaction. A control test was carried out likewise, without the addition of 2.0 g/L $NiFe_2O_4$.

### 1.5. Analytical methods

The COD of Fenton sludge was measured by the standard potassium dichromate method. The total iron content of the Fenton sludge and total iron leaching were determined using atomic absorption spectrometry (AAS, PinAAcle900T, PerkinElmer, America) after wet digestion. The synthesized $NiFe_2O_4$ was characterized using X-ray powder diffraction (XRD, D8 Advance, Bruker, Germany), a scanning electron microscope (SEM, JSM-6380, JEOL, Japan) equipped with an Energy dispersive spectrometer (EDS) system, Fourier transform infrared spectroscopy (FT-IR, Thermo Scientific, Nicolet iS10, USA) and Raman spectroscopy (LabRAM Aramis, Horiba Jobin Yvon, France). XRD recorded in the 2θ range from 20° to 80° was obtained with a Philips X-Pert diffractometer using Cu Kα radiation. FT-IR was collected in the region from 500 to 4000 $cm^{-1}$ at room temperature using a Nicolet iS10 spectroscopy on KBr pellets. Raman measurements were carried out in backscattering geometry using an Ar + excitation source having wavelength of 488 nm coupled with a Labram-HR800 micro-Raman spectrometer equipped with a ×50 objective, appropriate edge filter and peltier cooled charge coupled device detector. Magnetic properties were measured using a vibrating sample magnetometer (Lake Shore 7410, Lake Shore Cryotronics, Inc. USA) at room temperature. Phenol was identified and quantified by high performance liquid chromatography (HPLC) (Waters 2996, Waters Incorporation, USA) through use of an authentic standard and ultraviolet visible (UV–vis) spectroscopy analysis. The HPLC analysis was conducted at room temperature using a Waters RP18 column (5 μm, 4.6 mm × 250 mm) and a UV–vis detector. The mobile phase was a mixture of 45% methanol and 55% water pumped at a flow rate of 1.00 mL/min. The analysis was performed at 254 nm, with column temperature at 35°C.

## 2. Results and discussion

### 2.1. Characterization of synthesized particles

In this study, the precipitate obtained through the co-precipitation method was dried in the vacuum oven at 100°C for 8 hr and then sintered at 800°C for 6 hr. The obtained particles appeared reddish brown in color. The morphology and surface element distribution of the sample was investigated by SEM/EDS. As shown in Fig. 1a, the SEM micrograph demonstrated that the obtained sample was composed of irregular brick-like particles with a size of 2–8 μm, which was consistent with a previous study (Jia et al., 2012). The EDS analysis revealed that the products mainly contained three elements, i.e., O, Fe and Ni (Fig. 1b). The mass ratio of Ni:Fe:O was 25.38%:44.33%:30.28%. Correspondingly, the mole ratio of Ni:Fe:O was equal to 1:2.19:4.06, approximately to 1:2:4. Therefore, the stoichiometry of the obtained particles conformed to $NiFe_2O_4$.

The phase and crystalline properties of the calcined sample were further analyzed by XRD, as presented in Fig. 2. Apart from the most intense line at 2θ = 35.691°, which corresponded to the (311) plane of $NiFe_2O_4$, other lines were observed at 2θ = 30.301°, 37.331°, 43.381°, 53.831°, 57.381°, 62.021° and 74.581°, corresponding to the planes (200), (222), (400), (422), (511), (440) and (533), respectively. All of the detectable peaks indicated that the obtained $NiFe_2O_4$ has an inverse spinel structure, which was confirmed by the good agreement with the standard data (44-1485 IC DD; JCPDS) (Sailer and McCarthy, 1992). The absence of any additional lines confirmed the impurity-free characterization of $NiFe_2O_4$ phase. Hence, $NiFe_2O_4$ with an inverse spinel structure and with low impurity levels was obtained in this study, which was in good consistency with the EDS results shown in Fig. 1b.

The synthesized $NiFe_2O_4$ was also characterized by Raman spectroscopy (Fig. 3), which has been widely used to identify the microscopic vibrations caused by structural disorder. $NiFe_2O_4$ crystallizes in a spinel structure with space group $O^7h$ (Fd3 m), and theoretical group calculations yield five Raman active bands ($A_{1g} + E_g + 3F_{2g}$) (Kreisel et al., 1998; Ahlawat et al., 2011). In this structure, the tetrahedral (A) sites are occupied by one half of the $Fe^{3+}$ ions, whereas the other half of the $Fe^{3+}$

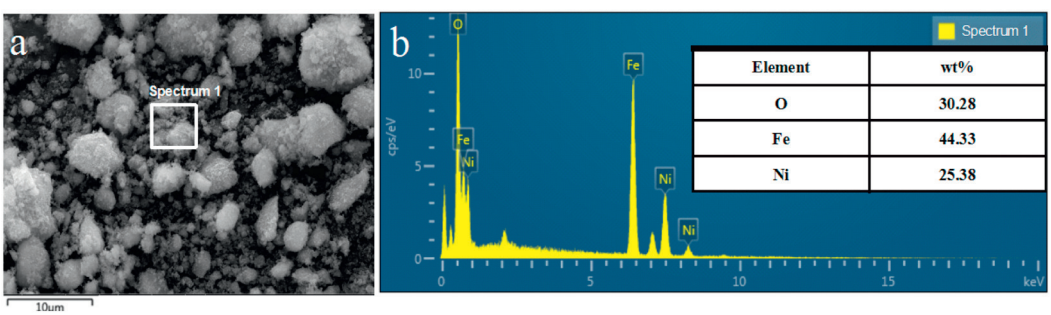


**Fig. 1 – Scanning electron microscope (SEM) image (a) and energy dispersive spectrometer (EDS) spectrum (b) of synthesized $NiFe_2O_4$.**

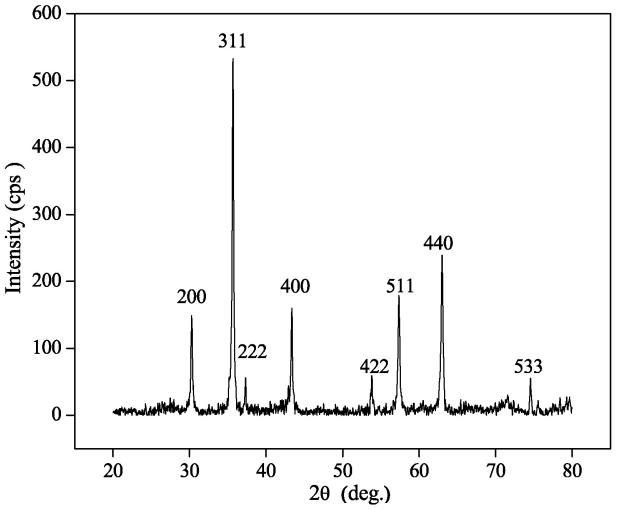


**Fig. 2 – X-ray powder diffraction (XRD) pattern of synthesized $NiFe_2O_4$.**

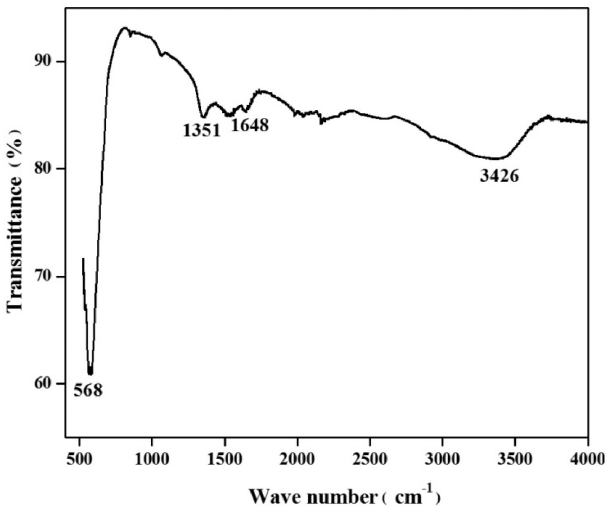


**Fig. 4 – Fourier transform infrared (FT-IR) spectrum of synthesized $NiFe_2O_4$.**

and $Ni^{2+}$ ions are distributed over the octahedral B sites. The $A_{1g}$ mode is due to the symmetric stretching of oxygen atoms along the Fe–O bonds in tetrahedral coordination. The $E_g$ mode originates from the symmetric bending of oxygen with respect to Fe, and the $F_{2g}(3)$ mode is caused by the asymmetric bending of oxygen. The $F_{2g}(2)$ mode is due to the asymmetric stretching of Fe and O. $F_{2g}(2)$ and $F_{2g}(3)$ modes correspond to vibrations of the octahedral group. The $F_{2g}(1)$ mode is assigned to the translational movement of $FeO_4$ (Fe at the tetrahedral site along with four oxygen atoms). Each peak can be presented as a doublet. At the microscopic level, the structure of $NiFe_2O_4$ can be considered as a mixture of two sublattices, with $Fe^{3+}$ and $Ni^{2+}$ believed to be ordered over the octahedral B sites. As depicted in Fig. 3, the peaks at 210, 327, 482, 567, and 695 $cm^{-1}$ corresponded to the $F_{2g}(1)$, $E_g$, $F_{2g}(2)$, $F_{2g}(3)$, and $A_g$ vibration modes, respectively. All the Raman peaks observed can be assigned to $NiFe_2O_4$.

Previous studies have indicated that there are two characteristic bands in the FT-IR spectrum for all spinels, particularly for ferrites (Salavati-Niasari et al., 2009), as indicated in Fig. 4. The highest band $\upsilon_1$, observed from 600 $cm^{-1}$ to 550 $cm^{-1}$, corresponds to the intrinsic stretching vibrations of the metal at the tetrahedral site Mtetra-O. The lowest band $\upsilon_2$, which is observed from 450 $cm^{-1}$ to 385 $cm^{-1}$, corresponds to the octahedral-metal stretching Mocta-O (Mouallem-Bahout et al., 2005). The strongest absorption band was located at 568 $cm^{-1}$, which was assigned to tetrahedral metal stretching vibrations. The absorption peaks at 3426 and 1648 $cm^{-1}$ were assigned to the stretching and bending vibrations of surface hydroxyl groups (Mouallem-Bahout et al., 2005). The result agreed well with the data from the literature (Liu et al., 2012), as well as XRD and Raman results.

The magnetic hysteresis loop of the synthesized $NiFe_2O_4$ is indicated in Fig. 5. The curves represented the non-overlapped type, which was in good accord with the typical mode for soft magnetic materials, indicating the ferrimagnetic behavior of the $NiFe_2O_4$. This magnetic characteristic made it possible to allow easy separation using an external magnet for possible reuse (Salavati-Niasari et al., 2009; Huo and Wei, 2009). The coercivity and saturation magnetization were 201.6 Oe and 28.9 μ/g, respectively. The reported saturation magnetization

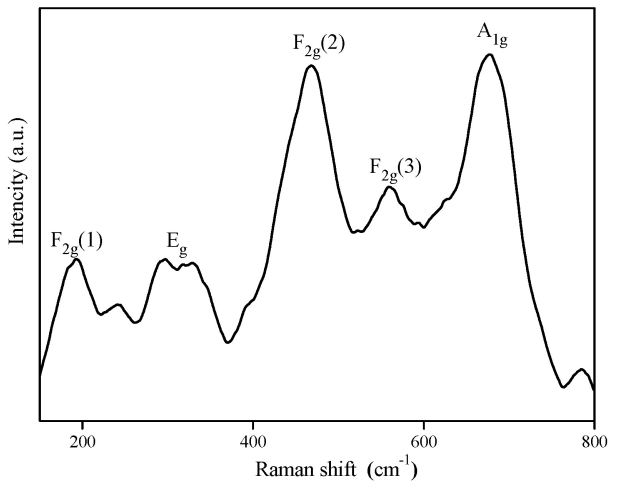


**Fig. 3 – Raman spectrum of synthesized $NiFe_2O_4$.**

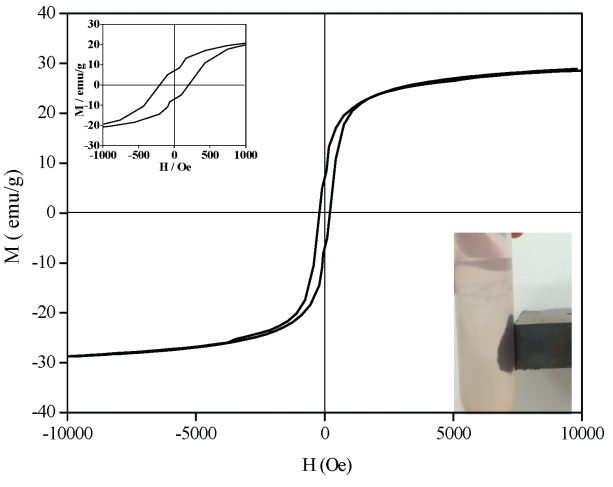


**Fig. 5 – Hysteresis loop for the $NiFe_2O_4$ at room temperature.**

was 46.5 emu/g (Zhang et al., 2015), which was higher than that of $NiFe_2O_4$ synthesized in this study. This phenomenon could be explained by the non-collinear spin arrangement near the surface of the $NiFe_2O_4$ particles (Salavati-Niasari et al., 2009). The low saturation magnetization confirmed that the synthesized particles were microparticles, which was in agreement with the SEM observations. The magnetic separability was tested in water by placing a magnet beside the centrifuge tube. The gray-black powders were attracted toward the magnet (the inset in Fig. 5), directly demonstrating the excellent separation properties of the obtained $NiFe_2O_4$ particles.

### 2.2. Heterogeneous Fenton degradation of phenol catalyzed by $NiFe_2O_4$

Recently, various magnetic materials have emerged as a useful class of heterogeneous catalysts, owing to their easy separation by application of an external magnetic field (Laurent et al., 2008; Lee et al., 2006). In this study, the catalytic properties of the obtained $NiFe_2O_4$ in Fenton system were tested, using phenol as the model contaminant.

As shown in Fig. 6, the phenol removal efficiency by $H_2O_2$ oxidation alone, i.e., with $H_2O_2$ but without $NiFe_2O_4$, was as low as 5.9% ± 0.1% within a reaction time of 330 min, which indicated that the contribution of $H_2O_2$ oxidation was negligible. In the system with $NiFe_2O_4$ but without $H_2O_2$, the phenol removal efficiency was 13.5% ± 0.4% within a reaction time of 330 min, probably due to the adsorption of phenol by $NiFe_2O_4$. However, phenol removal efficiency as high as 95.0% ± 3.4% could be achieved within the reaction time of 330 min in the presence of both $NiFe_2O_4$ and $H_2O_2$. Meanwhile, it could be seen that TOC removal increased with the increase of reaction time, as shown Fig. 7. TOC removal reached 49.4% ± 1.4% within the reaction time of 330 min. However, no insignificant improvement in terms of TOC removal was observed with the further increase of reaction time. From the data on phenol removal and TOC removal during the heterogeneous Fenton process, it could be inferred that phenol removal were mainly dominated by $H_2O_2$ oxidation catalyzed by $NiFe_2O_4$. Unfortunately, the identification of intermediates during phenol degradation was not successful in this study. This might be due to very low

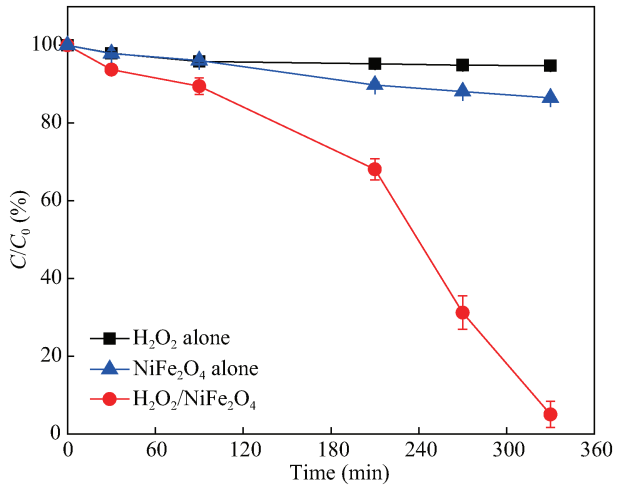


**Fig. 6 – The degradation of phenol under various conditions.**

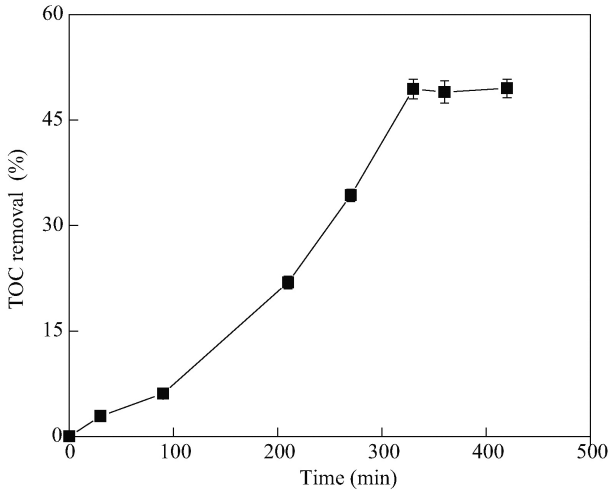


**Fig. 7 – The total organic carbon (TOC) removal in $NiFe_2O_4$/$H_2O_2$ system under optimal conditions.**

concentrations of the intermediates in the experiments, which needs further investigation.

Liu et al. (2012) have used $NiFe_2O_4$ as a heterogeneous photo-Fenton catalyst for the degradation of rhodamine B at the presence of oxalic acid. The results showed that the degradation efficiency of rhodamine B was as high as 98.7% in the reaction system with the addition of 4 g/L $NiFe_2O_4$ and under irradiation for 60.0 min. Magnetite $Fe_3O_4$, another representative spinel ferrite, has been used as a heterogeneous catalyst in the Fenton oxidation system for the removal of phenol (Minella et al., 2014). Almost complete degradation of 10 mg/L phenol could be achieved with optimal loading of 0.2 g/L $Fe_3O_4$ within 240 min. Sun et al. (2014) found that complete carbamazepine degradation could be achieved with the addition of 1.0 g/L of nano-$Fe_3O_4$ and 100 mmol/L of $H_2O_2$ at the presence of nitrilotriacetic acid. In this study, the removal efficiency of 250 mg/L phenol was as high as 95.0% ± 3.4% within 330 min with the addition of 2 g/L $NiFe_2O_4$ as Fenton catalyst. Compared to the above-mentioned studies, the $NiFe_2O_4$ synthesized in this study exhibited excellent catalytic performance in the heterogeneous Fenton process. Therefore, the $NiFe_2O_4$ prepared using Fenton sludge as an iron source could be applied in the Fenton process, demonstrating that the method for reuse of Fenton sludge proposed in this study merits investigation in consideration of the minimization and reduction of Fenton sludge.

### 2.3. The role of the leached iron ions in Fenton process

Due to the acid conditions used in the heterogeneous Fenton process, the leaching of iron ion from the $NiFe_2O_4$ particles was inevitable. During the heterogeneous Fenton degradation of phenol catalyzed by $NiFe_2O_4$ prepared in this study, the leached iron amounted to 6.3% ± 0.2% of total iron. In addition, the recovery ratio of $NiFe_2O_4$ catalyst in this study was found to be 97.1% ± 1.7%. Liu et al. (2012) investigated the performance of magnetic $NiFe_2O_4$ as a heterogeneous photo-Fenton catalyst for the degradation of Rhodamine B, and found that 4.0% of total iron was leached after the photo-Fenton reaction. The leached iron concentration was as high as 40.2 mg/L in a report on a Fenton reaction using iron oxide nanoparticles as catalyst

(Giraldi et al., 2009). The comparable leaching of iron and high recovery ratio of $NiFe_2O_4$ in this study indicated that the synthesized $NiFe_2O_4$ was relatively stable.

The leached iron could be an alternative Fenton catalyst in the heterogeneous Fenton reaction. Therefore, the contribution of a homogeneous Fenton reaction catalyzed by the leached iron was analyzed. As shown in Fig. 8, phenol degradation in the heterogeneous system catalyzed by the $NiFe_2O_4$ was found to be much faster than that in the homogeneous system catalyzed by the leached iron. Three hundred and thirty minutes later, phenol removal efficiency in the homogeneous Fenton system was as low as 13.5% ± 1.3%. However, phenol removal efficiency in the heterogeneous Fenton system reached as high as 95.0% ± 3.4%, which was about 6 times higher than that in the homogeneous Fenton system. These results confirmed that the heterogeneously initiated reaction predominated in the system, despite the contribution of leached iron to phenol degradation to some extent.

### 2.4. The reaction mechanism

Spinel ferrites have been used as heterogeneous Fenton catalysts for the degradation of various organics (Wang et al., 2014; Nguyen et al., 2011). However, the mechanism involved in Fenton-like catalytic oxidation reaction by spinel ferrites is still far from being fully understood. For the heterogeneous Fenton process, the most popular hypothesis in terms of $H_2O_2$ decomposition in the presence of $\equiv Fe^{II}$ or $\equiv Fe^{III}$ can be described by the following reactions:

$$\equiv Fe^{II} + H_2O_2 \rightarrow \equiv Fe^{III} + HO^{\cdot} + OH^- \quad (1)$$

$$\equiv Fe^{III} + H_2O_2 \rightarrow \equiv Fe^{II} + HO_2^{\cdot} + OH^+ \quad (2)$$

According to Reaction (1), $\equiv Fe^{II}$ could be readily converted to $\equiv Fe^{III}$, with HO. being generated. $\equiv Fe^{III}$ could act as an alternative catalyst for $H_2O_2$ decomposition, with generation of $\equiv Fe^{II}$ and $HO_2$.. However, the conversion of $\equiv Fe^{III}$ to $\equiv Fe^{II}$ was found to be much slower than the conversion of $\equiv Fe^{II}$ to $\equiv Fe^{III}$ (Chen et al., 2011; Wang et al., 2014), which negatively affected the Fenton efficiency. However, the situation would be different in a Fenton system catalyzed by spinel. Kulkarni et al. (2014) indicated that there exists a rapid electron exchange between $=M^{II}$ and $=N^{III}$ ions in the spinel structure. In the heterogeneous Fenton process catalyzed by $NiFe_2O_4$, a rapid electron exchange between $=Ni^{II}$ and $=Fe^{III}$ ions in the spinel structure would result in the rapid generation of $Fe^{2+}$, which could be beneficial for the Fenton reaction.

Therefore, the following mechanism for the Fenton reaction catalyzed by $NiFe_2O_4$ could be proposed, as indicated in Fig. 9. On the one hand, the $Fe^{3+}$ on the surface of $NiFe_2O_4$ particles, noted as $=Fe^{III}$, could react with the $H_2O_2$ to induce a heterogeneous Fenton reaction. In addition, the easy electron exchange between $=Ni^{II}$ and $=Fe^{III}$ in the $NiFe_2O_4$ would accelerate the conversion of $=Fe^{III}$ to $=Fe^{II}$, improving the catalytic efficiency. On the other hand, the dissolved Fe would mainly be in the form of $Fe^{3+}$ due to the presence of $H_2O_2$, which could take part to the homogeneous Fenton reaction. The HO. and $HO_2$. radical generated from the heterogeneous and homogeneous Fenton reactions could subsequently contribute to the removal of phenol.

## 3. Conclusions

A new reuse and disposal method of Fenton sludge was explored in this work. The magnetic spinel $NiFe_2O_4$ was successfully synthesized using iron-containing Fenton sludge as an iron source. In the phenol degradation process, phenol removal by $H_2O_2$ oxidation could be significantly accelerated at the presence of the synthesized $NiFe_2O_4$, indicating the excellent catalytic performance of $NiFe_2O_4$ in the heterogeneous Fenton process. Notably, a rapid electron exchange between $-Ni^{II}$ and $-Fe^{III}$ ions in $NiFe_2O_4$ could be beneficial for Fenton reaction. The synthesized $NiFe_2O_4$ catalyst was relatively stable, highly active and recoverable, and has potential applications in organic pollutant removal.

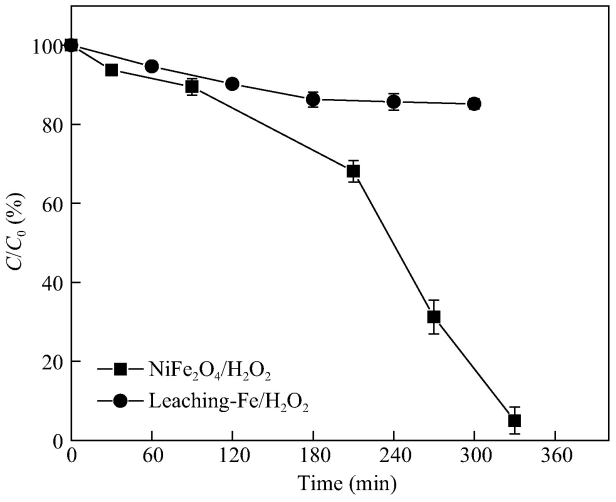


**Fig. 8 – The role of leached Fe during the Fenton degradation of phenol.**

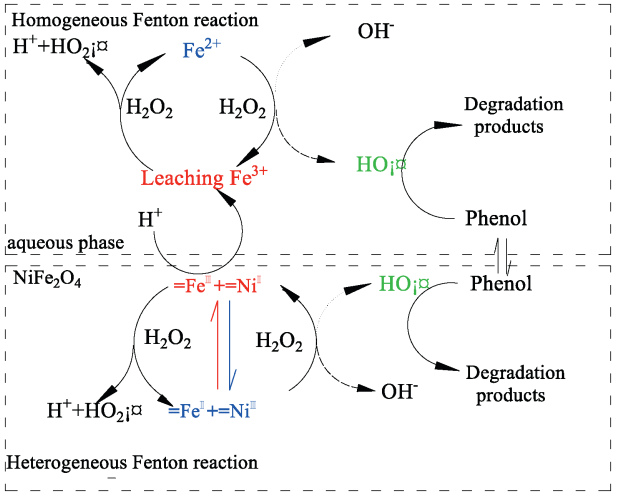


**Fig. 9 – Proposed mechanism involved in Fenton catalyzed by $NiFe_2O_4$.**

## Acknowledgments

This research is supported by the Major Project of Water Pollution Control and Management Technology of China (No. 2012ZX07101-003-001) and the Fundamental Research Funds for the Central Universities (No. 30916011312).

## REFERENCES

Ahlawat, A., Sathen, V.G., Reddy, V.R., Mossbauer, G.A., 2011. Mossbauer, Raman and X-ray diffraction studies of superparamagnetic $NiFe_2O_4$ nanoparticles prepared by sol–gel auto-combustion method. J. Magn. Magn. Mater. 323 (15), 2049–2054.

Aleksić, M., Kušić, H., Koprivanac, N., Leszczynska, D., Božić, A.L., 2010. Heterogeneous Fenton type processes for the degradation of organic dye pollutant in water-the application of zeolite assisted AOPs. Desalination 257 (1–3), 22–29.

Bautista, P., Mohedano, A.F., Casas, J.A., Zazo, J.A., Rodriguez, J.J., 2008. An overview of the application of Fenton oxidation to industrial wastewaters treatment. J. Chem. Technol. Biotechnol. 83 (10), 1323–1338.

Bolobajev, J., Kattel, E., Viisimaa, M., Goi, A., Trapido, M., Tenno, T., et al., 2014. Reuse of ferric sludge as an iron source for the Fenton-based process in wastewater treatment. Chem. Eng. J. 255, 8–13.

Cao, G., Sheng, M., Niu, W., Fei, Y., Li, D., 2009. Regeneration and reuse of iron catalyst for Fenton-like reactions. J. Hazard. Mater. 172 (2–3), 1446–1449.

Chen, L., Ma, J., Li, X., 2011. Strong enhancement on Fenton oxidation by addition of hydroxylamine to accelerate the ferric and ferrous iron cycles. Environ. Sci. Technol. 45 (9), 3925–3930.

Garrido-Ramirez, E.G., Theng, B.K., Mora, M.L., 2010. Clays and oxide minerals as catalysts and nanocatalysts in Fenton-like reactions—a review. Appl. Clay Sci. 47 (3–4), 182–192.

Giannakopoulou, T., Kompotiatis, L., Kontogeorgakos, A., Kordas, G., 2002. Microwave behavior of ferrites prepared via sol gel method. J. Magn. Magn. Mater. 246, 360–365.

Giraldi, T.R., Arruda, C.C., da Costa, G.M., Longo, E., Ribeiro, C., 2009. Heterogeneous Fenton reactants: a study of the behavior of iron oxide nanoparticles obtained by the polymeric precursor method. J. Sol-Gel Sci. Technol. 52, 299–303.

Hasmonay, E., Depeyrot, J., Sousa, M.H., Tourinho, F.A., Bacri, J.C., Perzynski, R., et al., 2000. Magnetic and optical properties of ionic ferrofluids based on nickel ferrite nanoparticles. J. Appl. Phys. 88 (11), 6628–6635.

Huo, J., Wei, M., 2009. Characterization and magnetic properties of nanocrystalline nickel ferrite synthesized by hydrothermal method. Mater. Lett. 63 (13–14), 1183–1184.

Ji, F., Li, C., Zhang, J., Deng, L., 2011. Efficient decolorization of dye pollutants with $LiFe(WO_4)_2$ as a reusable heterogeneous Fenton-like catalyst. Desalination 269 (1–3), 284–290.

Jia, Z., Peng, K., Xu, L., 2012. Preparation, characterization and enhanced adsorption performance for Cr(VI) of mesoporous $NiFe_2O_4$ by twice pore-forming method. Mater. Chem. Phys. 136 (2–3), 512–519.

Kreisel, J., Lucazeau, G., Vincent, H., 1998. Raman spectra and vibrational analysis of $BaFe_{12}O_{19}$ hexagonal ferrite. J. Solid State Chem. 137, 127–137.

Kulkarni, A.M., Desai, U.V., Pandit, K.S., Kulkarni, M.A., Wadgaonkar, P.P., 2014. Nickel ferrite nanoparticles–hydrogen peroxide: a green catalyst-oxidant combination in chemoselective oxidation of thiols to disulfides and sulfides to sulfoxides. RSC Adv. 4, 36702–36707.

Laurent, S., Forge, D., Port, M., Roch, A., Robic, C., Elst, L.V., 2008. Magnetic iron oxide nanoparticles: synthesis, stabilization, vectorization, physicochemical characterizations and biological applications. Chem. Rev. 108 (6), 2064–2110.

Lee, D., Lee, J., Lee, H., Jin, S., Hyeon, T., Kim, B.M., 2006. Filtration-free recyclable catalytic asymmetric dihydroxylation using a ligand immobilized on magnetic mesocellular mesoporous silica. Adv. Synth. Catal. 348 (1–2), 41–46.

Liu, J., Ou, C., Han, W., Faheem, Shen, J., Bi, H., et al., 2015. Selective removal of nitroaromatic compounds from wastewater in an integrated zero valent iron (ZVI) reduction and $ZVI/H_2O_2$ oxidation process. RSC Adv. 5 (71), 57444–57452.

Liu, S.Q., Feng, L.R., Xu, N., Chen, Z.G., Wang, X.M., 2012. Magnetic nickel ferrite as a heterogeneous photo-Fenton catalyst for the degradation of rhodamine B in the presence of oxalic acid. Chem. Eng. J. 203, 432–439.

Ma, X., Xia, H., 2009. Treatment of water-based printing ink wastewater by Fenton process combined with coagulation. J. Hazard. Mater. 162 (1), 386–390.

Minella, M., Marchetti, G., De Laurentiis, E., Malandrino, M., Maurino, V., Minero, C., et al., 2014. Photo-Fenton oxidation of phenol with magnetite as iron source. Appl. Catal. B Environ. 154, 102–109.

Mouallem-Bahout, M., Bertrand, S., Peňa, O., 2005. Synthesis and characterization of $Zn_{1-x}Ni_xFe_2O_4$ spinels prepared by a citrate precursor. J. Solid State Chem. 178 (4), 1080–1086.

Navalon, S., Alvaro, M., Garcia, H., 2010. Heterogeneous Fenton catalysts based on clays, silicas and zeolites. Appl. Catal. B Environ. 99 (1–2), 1–26.

Nguyen, T.D., Phan, N.H., Do, M.H., Ngo, K.T., 2011. Magnetic $Fe_2MO_4$ (M:Fe,Mn) activated carbons: fabrication, characterization and heterogeneous Fenton oxidation of methyl orange. J. Hazard. Mater. 185 (2–3), 653–661.

Pignatello, J.J., Oliveros, E., Mackay, A., 2006. Advanced oxidation processes for organic contaminant destruction based on the Fenton reaction and related chemistry. Crit. Rev. Environ. Sci. Technol. 36 (1), 1–84.

Rashad, M.M., Fouad, O.A., 2005. Synthesis and characterization of nano-sized nickel ferrites from fly ash for catalytic oxidation of CO. Mater. Chem. Phys. 94 (2–3), 365–370.

Rezlescu, N., Iftimie, N., Rezlescu, E., Doroftei, C., Popa, P.D., 2006. Semiconducting gas sensor for acetone based on the fine grained nickel ferrite. Sensors Actuators B Chem. 114 (1), 427–432.

Sailer, R., McCarthy, G., 1992. ICDD Grant in Aid.

Saito, N., Sakamoto, H., Sugimoto, K., 1998. Crevice corrosion of austenitic alloys in high-temperature water. Corrosion 54 (9), 700–712.

Salavati-Niasari, M., Davar, F., Mahmoudi, T., 2009. A simple route to synthesize nanocrystalline nickel ferrite ($NiFe_2O_4$) in the presence of octanoic acid as a surfactant. Polyhedron 28 (8), 1455–1458.

Shen, J., Ou, C., Zhou, Z., Chen, J., Fang, K., Sun, X., et al., 2013. Pretreatment of 2,4-dinitroanisole (DNAN) producing wastewater using a combined zero-valent iron (ZVI) reduction and Fenton oxidation process. J. Hazard. Mater. 260, 993–1000.

Sheu, S., Weng, H., 2001. Treatment of olefin plant spent caustic by combination of neutralization and Fenton reaction. Water Res. 35 (8), 2017–2021.

Sun, S., Zeng, X., Li, C., Lemley, A.T., 2014. Enhanced heterogeneous and homogeneous Fenton-like degradation of carbamazepine by nano-$Fe_3O_4/H_2O_2$ with nitrilotriacetic acid. Chem. Eng. J. 244, 44–49.

Takbas, M., Yatmaz, H.C., Bektas, N., 2008. Heterogeneous photo-Fenton oxidation of reactive azo dye solutions using

iron exchanged zeolite as a catalyst. Microporous Mesoporous Mater. 115 (3), 594–602.
Wang, Y., Zhao, H., Li, M., Fan, J., Zhao, G., 2014. Magnetic ordered mesoporous copper ferrite as a heterogeneous Fenton catalyst for the degradation of imidacloprid. Appl. Catal. B Environ. 147, 534–545.
Yoo, H.C., Cho, S.H., Ko, S.O., 2001. Modification of coagulation and Fenton oxidation processes for cost-effective leachate treatment. J. Environ. Sci. Health A 36 (1), 39–48.
Zhang, Z., Yao, G., Zhang, X., Ma, J., Lin, H., 2015. Synthesis and characterization of nickel ferrite nanoparticles via planetary ball milling assisted solid-state reaction. Ceram. Int. 41 (3), 4523–4530.